Open Access Full Text Article

ORIGINAL RESEARCH

# Liposomes functionalized to overcome the blood–brain barrier and to target amyloid-β peptide: the chemical design affects the permeability across an in vitro model

Elisa Salvati
Francesca Re
Silvia Sesana
Ilaria Cambianica
Giulio Sancini
Massimo Masserini
Maria Gregori

Department of Health Sciences,
University of Milano-Bicocca,
Monza, Italy

**Purpose:** We investigated the ability of amyloid-β-targeting liposomes, decorated with an anti-transferrin receptor antibody, to cross the blood–brain barrier (BBB), comparing two antibody ligation techniques.

**Methods:** Fluorescent or radiolabeled liposomes composed of sphingomyelin/cholesterol and containing phosphatidic acid, known to bind amyloid-β, were further functionalized with the anti-transferrin receptor antibody RI7217. Two different techniques were used to attach RI7217 to the liposomes surface: biotin/streptavidin linkage or thiol–maleimide covalent ligation. Surface plasmon resonance (SPR) and immunoblotting were employed to assess the nanoparticles' binding performances. Confocal microscopy and radiochemical techniques were used for uptake and permeability studies on an in vitro BBB model made of human brain capillary endothelial cells hCMEC/D3.

**Results:** Immunoblotting experiments showed that RI7217-functionalized liposomes bind to transferrin receptor independently of the procedure employed to ligate their surface with the antibody, while SPR experiments showed a slightly higher affinity for covalently functionalized nanoliposomes. The functionalization with RI7217 did not affect the liposomes' affinity for amyloid-β. The functionalization of liposomes with RI7217, independently of the ligation procedure, gave higher values of uptake and permeability across the barrier model in comparison to the nondecorated ones, without cell monolayer alterations. Of note, the best performing particles were those covalently coupled with the antibody. The ratios of the two radiolabeled lipids ($^3$H-sphingomyelin and $^{14}$C-phosphatidic acid) present in the liposome bilayer were found to be similar in the apical and in the basolateral compartments of the barrier model, suggesting that liposomes were transported intact across the cell monolayer. Confocal experiments showed no co-localization of RI7217-liposomes with early/late endosomes or early lysosomes.

**Conclusion:** Our results suggest that RI7217 promotes the in vitro barrier crossing of liposomes containing phosphatidic acid, targeting the Alzheimer's disease amyloid-β peptide. Moreover, for the first time, we prove herein the superior efficiency of covalent coupling of RI7217 versus biotin/streptavidin ligation to facilitate liposomes in overcoming the BBB in vitro.

**Keywords:** liposomes, blood–brain barrier, amyloid-β peptide, RI7217, antibody conjugation, surface plasmon resonance

Correspondence: Francesca Re
Department of Health Sciences,
University of Milano-Bicocca,
via Cadore 48, 20900 Monza-Italy
Tel +39 026 448 8311
Fax +39 026 448 8068
Email francesca.re1@unimib.it

## Introduction

Approximately 24 million people worldwide suffer from dementia, of which 60% is due to Alzheimer's disease (AD). AD incidence is 0.4% for individuals aged 65–69 years and increases to 10% for those over 90 years.[1] AD is characterized clinically

by learning and memory impairment and pathologically by neuronal loss, primarily due to intracellular neurofibrillary tangles and extracellular amyloid plaques, mainly composed of aggregates of amyloid-β peptides (Aβ).[2] The delivery of drugs to the central nervous system (CNS) is limited by the existence of the blood–brain barrier (BBB), and this poses limitations for the treatment and diagnosis of brain disorders.[3] The use of properly designed nanoparticles represents a promising strategy by which to successfully enhance the CNS penetration of therapeutics relying on the possibility of surface multifunctionalization, potentially allowing both targeting of Aβ and BBB crossing, thus making them suitable for therapy and/or diagnosis of AD.[4–9]

Within this framework, we recently designed liposomes (LIP) functionalized with phosphatidic acid (PA-LIP) that demonstrated very high affinity for Aβ[10] and that were able to rescue cells from Aβ toxicity in vitro.[11] In the present investigation, we functionalized PA-LIP with a possible promoter of BBB crossing, the antibody RI7217 against the transferrin receptor (TfR). TfR targeting has been suggested as a possible strategy by which nanoparticles can reach the brain,[12] given its expression on the BBB endothelial cells for the regulation of brain uptake of iron.[13]

To attach RI7217 antibodies to nanoparticle surfaces,[14–16] we employed biotin/streptavidin (b/s) ligation or thiol–maleimide covalent coupling to assess whether the chemical design may influence the biological performance. In particular, we examined their uptake by immortalized human brain capillary endothelial cells (hCMEC/D3) and their permeability across an in vitro BBB model made with the same cells. To the best of our knowledge, whether the ligation procedure of antibodies affects these features has not yet been studied.

# Materials and methods
## Materials
All chemical reagents were from Sigma-Aldrich (St Louis, MO, USA). Bovine brain sphingomyelin (Sm), cholesterol (Chol), 1,2-Dimyristoyl-sn-glycero-3-phosphatidic acid (PA), 1,2-distearoyl-sn-glycero-3-phospho-ethanolamine-N-[maleimide(polyethyleneglycol)-2000] (PE-PEG-mal), and 1,2-distearoyl-sn-glycerol-3-phosphoethanolamine-N-[biotinyl(polyethyleneglycol)-2000] (PE-PEG-biotin), were purchased from Avanti Polar Lipids, Inc (Alabaster, AL, USA). N-(4,4-difluoro-5,7-dimethyl-4-bora-3a,4a-diaza-s-indacene-3-dodecanoyl)sphingosyl-phosphocholine (BODIPY-Sm) was from Molecular Probes (Life Technologies, Carlsbad, CA, USA). Aβ1-42 peptide (Aβ), N-acetyl-L-

cysteine, streptavidin, Sepharose CL-4B, and Triton X-100 were purchased from Sigma-Aldrich. [$^3$H]-Sm and [$^{14}$C]-PA were from PerkinElmer (Waltham, MA, USA). Amicon Ultra-15 centrifugal 10K filter devices and polycarbonate filters for extrusion procedure were purchased from Merck Millipore (Billerica, MA, USA). The Thermobarrel Extruder was from Lipex Biomembranes (Vancouver, BC, Canada). Purified rat anti-mouse RI7217 and the biotinylated antibody were from BioLegend (San Diego, CA, USA). Nonspecific mouse immunoglobulin G2a (IgG2a) was from AbD Serotec (now Bio-Rad Laboratories, Hercules, CA, USA). Recombinant mouse TfR was from Sino Biological Inc (Beijing, People's Republic of China). All media and supplements for cell cultures and phalloidin were supplied by Life Technologies.

## Preparation of RI7217-PA-LIP
### Preparation of LIP
LIP were composed of a matrix of Sm/Chol/PA (PA-LIP) (47.5:47.5:5 molar ratio) as previously described,[10] and mixed or not with PE-PEG-biotin (for b/s ligation) or PE-PEG-mal (for covalent coupling) ranging from 0.05 to 1 % mol. For preparation of fluorescently labeled LIP, 0.5 molar % of total Sm was substituted with BODIPY-Sm. For in vitro studies of cellular uptake and permeability, 0.001 molar % of [$^3$H]-Sm (100 µCi/mL) and 0.002 molar % of [$^{14}$C]-PA (50 µCi/mL), were added as tracers to follow lipid distribution by radioactivity counting. LIP were prepared in 10 mM phosphate-buffered saline (PBS), pH 7.4, by extrusion procedure through a 100 nm pore polycarbonate filters, as previously described.[10] Phospholipid recovery after extrusion was determined by phosphorous assay using the method of Stewart.[17]

### Functionalization of PA-LIP with RI7217 by b/s ligation technique
Biotinylated PA-LIP were incubated with 2.5-fold molar excess of streptavidin compared to surface exposed biotin for 1 hour at 25°C and then overnight at 4°C. Free streptavidin was removed by gel filtration (Sepharose 4B-CL column, 25 × 1 cm). Streptavidin-labeled LIP (at a lipid concentration of 4 mM) were then incubated with the biotinylated RI7217 at a molar ratio RI7217/phospholipids of 1:1000 at 25°C for 2 hours and then overnight at 4°C. Unbound antibody was removed by gel filtration (Sepharose 4B-CL column, 25 × 1 cm) and collected and quantified by ELISA technique, as already reported for similar antibodies.[18] It was not possible to directly quantify bound RI7217 because of the presence

of streptavidin on LIP. Thus, bound RI7217 was quantified indirectly from the unbound antibody. Briefly, polystyrene 96-well plates were coated with streptavidin (2 µg) for 16 hours at 4°C. After washing with PBS and blocking with 2% bovine serum albumin (BSA) (1 hour at 37°C), samples or known concentrations of biotinylated RI7217 (for quantification) were applied (1 hour at 37°C) and well plates were washed with PBS. Rabbit anti-mouse IgG labeled with peroxidase (Sigma-Aldrich) was added as a second antibody (at 1:2000 dilution in 1% BSA) for 1 hour at 37°C, and wells were washed with PBS (3 times) and 0.1 M citrate buffer and incubated at 25°C with 100 µL peroxidase substrate solution (0.06% $H_2O_2$ and 18.5 mM $o$-phenylenediamine) until color development (10 minutes). The reaction was stopped with sulfuric acid and OD-492 nM was measured. These LIP will be called b/s-RI-PA-LIP.

## Functionalization of PA-LIP with RI7217 by covalent coupling

To covalently bind RI7217 to maleimide-containing LIP, free thiol groups were generated by reacting the antibody with Traut's reagent in 0.15 M Na-borate buffer with 0.1 mM ethylenediaminetetraacetic acid (EDTA), pH 8.5, as described previously.[19] After incubation for 90 minutes at 25°C under $N_2$, RI7217 solution was concentrated and the buffer exchanged with PBS (pH 7.4) using an Amicon filter device. Ellman's reagent was used to determine the number of sulfhydryl groups on RI7217, using acetylcysteine for the calibration curve.[20] Using a RI7217/2-iminothiolane (Traut's reagent) molar ratio of 1:10, an average of 3 primary amines per antibody were thiolated. Thiolated RI7217 was then incubated with LIP (4 mM) containing PE-PEG-mal overnight at 25°C at a molar ratio RI7217/ phospholipids of 1:1000. To remove the unbound RI7217, the LIP suspension was passed through a Sepharose 4B-CL column (25 × 1 cm). The amount of RI7217 bound to LIP and unbound was quantified by Bradford assay.[21] Background absorbance values of buffer and control LIP without RI7217 were subtracted from sample absorbance values. Phospholipid recovery after gel-chromatography purification was determined as described above.[17] These LIP will be called cov-RI-PA-LIP.

# Characterization of RI-PA-LIP
## Physicochemical characterization of LIP
All LIP preparations were characterized in terms of size, ζ-potential, polydispersity index (PI) and stability by dynamic light scattering (DLS), as described previously.[10]

The reported data are the mean of at least five different measurements.

## Assessment of RI7217 binding to TfR by dot-blot procedure

The binding of chemically modified RI7217 and RI-PA-LIP to TfR was assessed by dot-blot procedure, modified from the previously described protocol.[22] Twenty nanograms of TfR were spotted on Polyvinylidene fluoride (PVDF) membranes, left to dry, and then incubated at 37°C for 30 minutes in 5% nonfat milk PBS solution. Membranes were incubated for 90 minutes at 25°C with 60 nM nonspecific mouse IgG2a or RI7217 or biotinylated RI7217 or thiolated RI7217 or b/s-RI-PA-LIP or cov-RI-PA-LIP diluted in nonfat milk PBS solution. After washing, the membranes were incubated with horseradish peroxidase (HRP)-conjugated secondary antibody for 2 hours at 25°C (anti-mouse 1:20000 dilution in nonfat milk PBS solution), followed by enhanced chemiluminescence detection (KODAK image station 2000R, PerkinElmer, Waltham, MA, USA).

## Assessment of LIP binding properties by surface plasmon resonance (SPR)

The binding properties of RI-PA-LIP for TfR and Aβ were assessed by SPR. A SensiQ semi-automatic instrument SensiQ Technologies (Oklahoma City, OK, USA) with two flow channels was employed. A COOH5 sensor chip (ICX Technologies) was installed in the system and TfR was immobilized on one channel using amine-coupling chemistry, while the other channel was used as reference surface. The sensor surface was activated by injecting 0.4 M (N-(3-Dimethylaminopropyl)-N′-ethylcarbodiimide hydrochloride) (EDC) and 0.1 M (N-Hydroxysuccinimide) ([NHS] 1:1, v/v) into the flow channels. TfR was diluted to 10 µg/mL in acetate buffer (pH 4.0) and injected for 2 minutes at a flow rate of 10 µL/minute. The unoccupied sites were blocked with 1 M ethanolamine (pH 8.0). The final immobilization level was ~6000 resonance units (RU, 1 RU = 1 pg/mm²). LIP were injected at concentrations of exposed RI7217 of 10, 30, 100, 300, and 600 nM at a flow rate of 30 µL/minute.

Aβ aggregates were prepared as already described[10] and immobilized on a second COOH5 sensor chip by the same procedure described previously.[23] The final immobilization level was ~5000 RU. LIP were injected at a flow rate of 30 µL/minute at two concentrations of total lipids (100 µM and 300 µM, corresponding to 2.5 µM and 7.5 µM of exposed PA). All procedures were performed at 25°C. Nonspecific

binding of LIP on the reference channel was automatically subtracted from the total signal. The observed data were fitted to the 1:1 association model and the dissociation constant (KD) was automatically obtained from the ratio between dissociation and association rate ($K_d/K_a$). The data analysis was carried out with Qdat Software (ICX Technologies) provided by the manufacturer.

## Uptake and transcytosis of RI-PA-LIP by human brain endothelial cells

### Cellular uptake of LIP by confocal microscopy

Immortalized hCMEC/D3 were provided by Institut National de la Santé et de la Recherche Médicale ([INSERM] Paris, France) and cultured as previously described.[24] Sixty-five thousand cells/cm^{2} were cultured for 2 days on rat type I collagen-coated cover slips (diameter 22 mm) positioned in culture dishes and then incubated with fluorescent LIP at 37°C for 2 hours. After that, cells were rinsed three times with PBS and fixed with a 10% formalin solution. Cells were permeabilized with 0.2% Triton-X100 in PBS for 15 minutes then rinsed twice and incubated with a solution of 1% phalloidin (staining actin filaments) in PBS for 1 hour, then with 20 μM 4′,6-diamidino-2-phenylindole ([DAPI] nuclear staining) in PBS for 10 minutes, and finally with antibodies against lysosomal-associated membrane protein 1 ([LAMP1] late endosome and early lysosome staining [1:200]) or EAA1 (early endosome staining [1:200]) for 4 hours at 25°C, as previously described.[24] A LSM710 inverted confocal laser scanning microscope equipped with a Plan-Neofluar 63×/1.4 oil objective (Carl Zeiss Meditec AG, Jena, Germany) was employed to assess the cellular uptake of LIP.

### Cellular uptake and permeability of LIP by radiochemical techniques

hCMEC/D3 cells (passages 25–35) were seeded on 12-well transwell inserts coated with type I collagen in a density of $5 \times 10^4$ cells/cm^{2} and cultured with 0.5 mL and 1 mL of culture medium in the upper and lower chamber, respectively. Cells were treated with LIP when the transendothelial electrical resistance (TEER) value (measured by EVOMX meter, STX2 electrode; World Precision Instruments, Sarasota, FL, USA) was found to be the highest. The functional properties of cell monolayers were assessed by measuring the endothelial permeability (EP) of [14C]-sucrose and [3H]-propranolol (between 0 and 120 minutes) as described previously.[25] Radiolabeled LIP (0.5 mL; from 100 to 400 nmols of total lipids/well) were added to the upper chamber and incubated for between 10 and 120 minutes. After these periods of

incubation, the radioactivity in the upper and lower chambers was measured by liquid scintillation counting to calculate the EP of LIP across the cell monolayers, taking account of their passage through the filter without cells.[25] After 2 hours, hCMEC/D3 cells were washed with PBS and detached from the transwell inserts with trypsin/EDTA for 15 minutes at 37°C. Cell-associated radioactivity was measured and the total lipid uptake calculated.

### Assessment of LIP cytotoxicity on hCMEC/D3 cells

hCMEC/D3 cells were grown on 12-well plates until confluence. Medium was replaced and LIP (400 nmols of total lipids) suspended in cell culture medium were incubated at 37°C with the cells for 24 hours. After treatment, the cell viability was assessed by ([3-(4,5-dimethylthiazol-2-yl)-2,5-diphenyltetrazolium bromide]) (MTT) assay, as described previously.[26] Each sample was analyzed at least in triplicate. Moreover, TEER and permeability of [14C]-sucrose were also determined in the presence of LIP to assess the effect of LIP on monolayer integrity.

## Statistical analysis

All experiments were carried out at least in triplicate. The differences were evaluated for statistical significance using the Student's *t*-test.

## Results

### Preparation and characterization of LIP

The total lipid recovery of LIP, prepared by extrusion procedure, was about 90% for all the samples. PA-LIP were functionalized with RI7217 by biotin/streptavidin ligation (Figure 1A) or by covalent coupling (Figure 1B); for both techniques, the RI7217 binding occurred at the PEG terminus of PE-PEG lipid inserted in LIP. Preparation conditions were optimized to couple 40–45 antibody molecules on the surface of each LIP, for both ligation methods used. To achieve this goal, different concentrations of PE-PEG-biotin (for b/s ligation) or PE-PEG-mal (for covalent coupling) were incorporated into LIP. The number of antibodies conjugated per LIP was based on the assumption that a 100 nM liposome contains ~100,000 molecules of phospholipids.[16] Optimal conditions were achieved with 0.1% (mol/mol of total lipids) of PE-PEG-biotin or with 1% of PE-PEG-mal. RI-PA-LIP resulted as monodispersed (PI = 0.1), negatively charged (−35 ± 1.2 mV for b/s-RI-PA-LIP and −32 ± 1.7 mV for cov-RI-PA-LIP) with a size of 129.3 ± 1.7 nM and 121.3 ± 2.3 nM for b/s-RI-PA-LIP and cov-RI-PA-LIP, respectively. All the preparations were stable in size up to 7 days (data not shown).
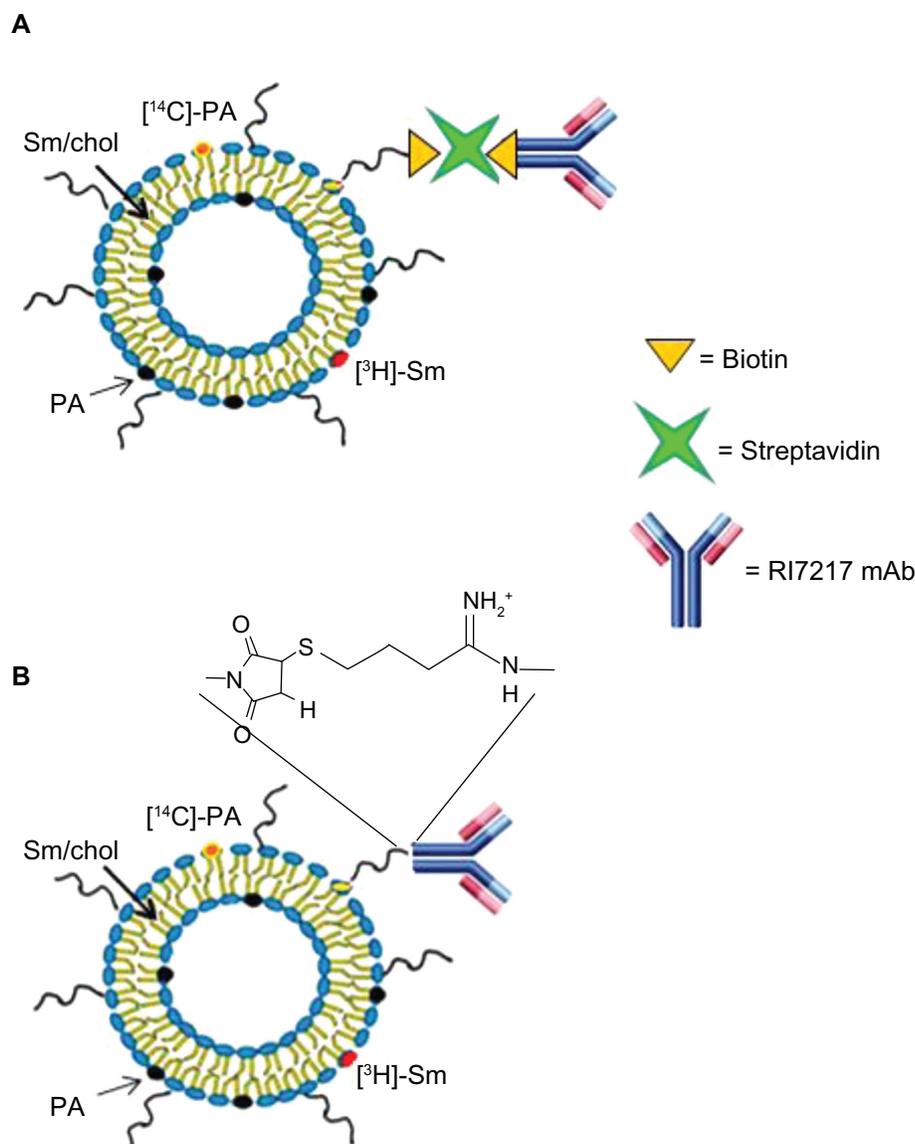
**Figure 1** Theoretical structure of RI-PA-LIP. RI7217 antibody was linked to LIP by (**A**) biotin/streptavidin ligation technique or (**B**) covalent coupling via thiol–maleimide reaction.
**Abbreviations:** Chol, cholesterol; LIP, liposomes; mAb, monoclonal antibody; [$^{14}$C]-PA, 14C-radiolabelled phosphatidic acid; [$^{3}$H]-Sm, tritiated sphingomyelin; PA, phosphatidic acid; Sm, sphingomyelin.
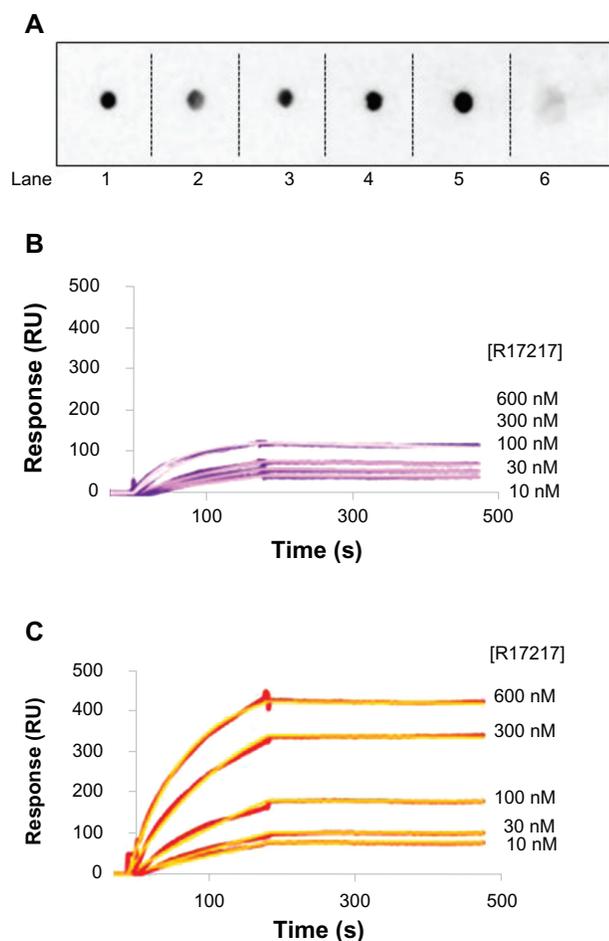
## Binding of RI-PA-LIP to TfR

The ability of RI7217 to bind its receptor, after chemical modifications and after coupling to LIP, was verified by immunoblotting and SPR techniques. Immunoblotting results showed that the thiolated or biotinylated RI7217, as well as RI7217 linked to PA-LIP, retained the ability of native antibody to bind TfR (Figure 2A). The binding affinity of RI-PA-LIP towards TfR was investigated by SPR. Representative sensorgrams are shown in Figure 2B and C. The KD, calculated by fitting the experimental data with a single binding site isotherm by Qdat Software analysis, were 2.5 nM for cov-RI-PA-LIP and 11.0 nM for b/s-RI-PA-LIP, calculated with respect to RI7217 exposed on the LIP surface.

## Binding of LIP to Aβ aggregates

The evaluation of binding affinity of LIP towards Aβ was carried out by using SPR. The KD were obtained by fitting the experimental data with a single binding site isotherm by Qdat Software analysis and were 48.5 nM for PA-LIP, in agreement with data previously reported,[10] 37.0 nM for cov-RI-PA-LIP, and 43.3 nM for b/s-RI-PA-LIP, calculated with respect to PA exposed on LIP surface (Figure 3).

## Cellular uptake of LIP investigated by confocal microscopy

Confocal microscopy images illustrate that the uptake of PA-LIP was higher after functionalization with RI7217

**Figure 2** Binding of LIP to TfR. (**A**) Dot blots of 20 ng TfR spotted in a PVDF membrane, incubated with cov-RI-PA-LIP (lane 1), or b/s-RI-PA-LIP (lane 2), or biotinylated RI7217 (lane 3), or thiolated RI7217 (lane 4), or native RI7217 (lane 5), or control IgG (lane 6). Spots were detected with HRP-conjugated IgG anti-mouse, followed by ECL detection. SPR sensorgrams resulting from the binding of (**B**) b/s-RI-PA-LIP or (**C**) cov-RI-PA-LIP on TfR covalently immobilized on the gold sensor surface.
**Note:** LIP were injected at concentrations of exposed RI7217 of 10 to 600 nM.
**Abbreviations:** b/s, biotin/streptavidin; cov, covalent; ECL, ; HRP, horseradish peroxidise; Ig, immunoglobulin; LIP, liposomes; PA, phosphatidic acid; PVDF, polyvinylidene fluoride; RI, RI7217 antibody; SPR, surface plasmon resonance; TfR, transferrin receptor.

(Figure 4). In particular, the uptake was higher for cov-RI-PA-LIP compared to b/s-RI-PA-LIP. Experiments designed to evaluate the intracellular localization of LIP showed that there was no colocalization with early endosomes or late endosomes and early lysosomes, for both LIP tested (Figure 5). LIP did not induce changes in actin organization of hCMEC/D3 cells.

## Cellular uptake and permeability of RI-PA-LIP investigated by radiochemical techniques

hCMEC/D3 cells, grown on transwell membrane inserts, were incubated with LIP on day 12, when the maximal
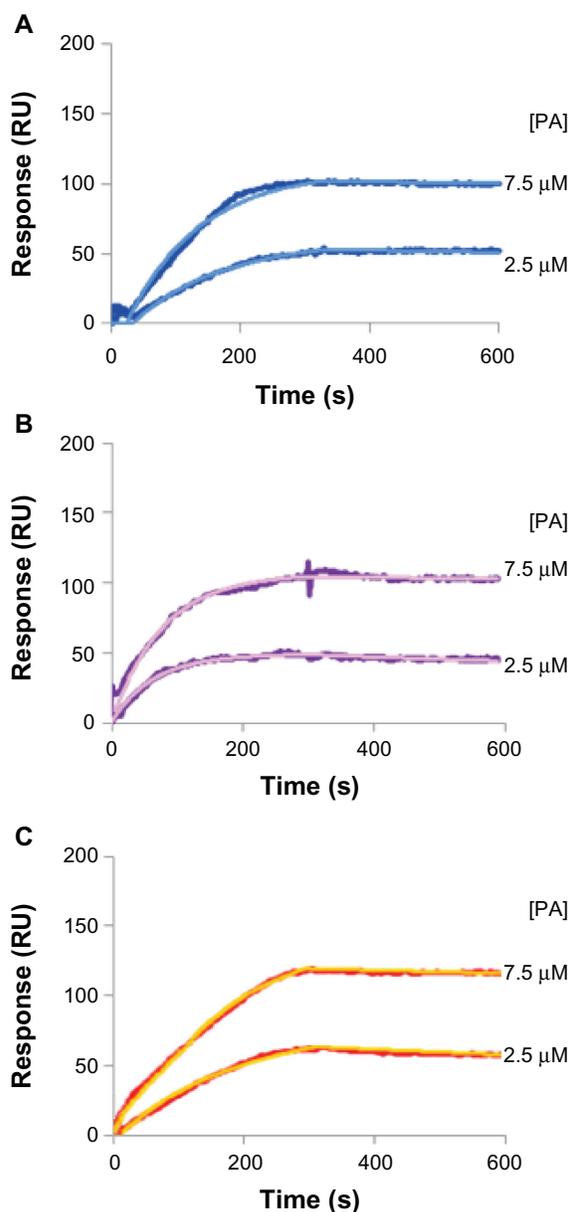


**Figure 3** Binding of LIP to Aβ fibrils. SPR sensorgrams resulting from the binding of (**A**) PA-LIP or (**B**) b/s-RI-PA-LIP or (**C**) cov-RI-PA-LIP on Aβ fibrils covalently immobilized on the gold sensor surface.
**Note:** LIP were injected at two concentrations of total lipids (100 μM and 300 μM), corresponding to 2.5 μM and 7.5 μM of exposed PA.
**Abbreviations:** Aβ, Aβ1-42 peptide; b/s, biotin/streptavidin; cov, covalent; LIP, liposomes; PA, phosphatidic acid; RI, RI7217 antibody; SPR, surface plasmon resonance.

TEER value was registered ($123 \pm 6 \; \Omega \cdot cm^2$). Transport of [$^{14}$C]-sucrose and [$^3$H]-propranolol was measured, with EP values of $1.48 \times 10^{-3}$ cm/minute and $3.51 \times 10^{-3}$ cm/minute, respectively, in agreement with the values reported in literature.[27] Different amounts of LIP were added in the upper compartment and the radioactivity uptaken from the cells after 2 hours of incubation was measured. As shown in Figure 6A, the amount of radioactivity uptaken increased by increasing the
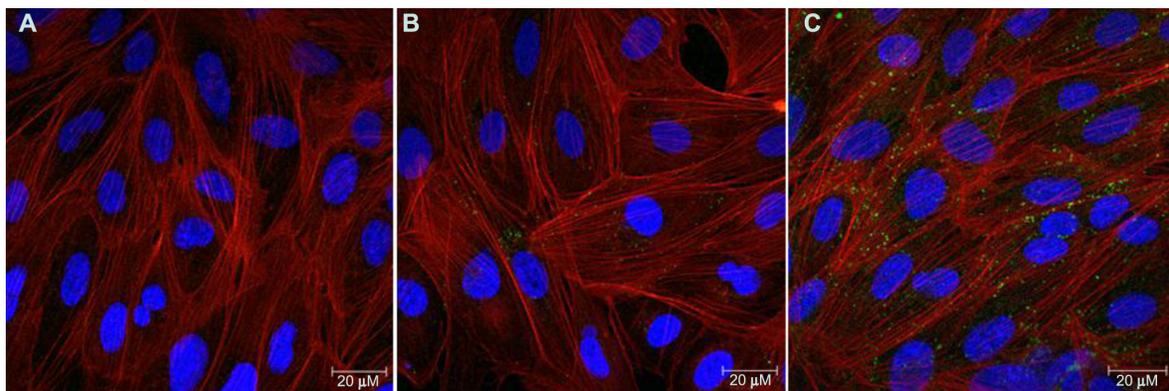
**Figure 4** CLSM of hCMEC/D3 cells after incubation with LIP. hCMEC/D3 cells were incubated with fluorescent labeled LIP (200 nmols of total lipids) for 2 hours at 37°C, 5% $CO_2$ saturation. hCMEC/D3 cells after incubation with (**A**) PA-LIP, (**B**) LIP b/s-RI-PA-LIP, or (**C**) cov-RI-PA-LIP.
**Notes:** Cells were incubated with phalloidin in order to visualize the actin filaments (red fluorescence); nuclear staining was performed by DAPI (blue staining) and BODIPY-Sm to mark LIP (green staining). Scale bar = 20 μM.
**Abbreviations:** b/s, biotin/streptavidin; BODIPY, boron-dipyrromethene; CLSM, ; cov, covalent; DAPI, 4′,6-diamidino-2-phenylindole; LIP, liposomes; PA, phosphatidic acid; CLSM, confocal laser scanning microscopy; RI, anti-transferrin receptor RI7217 antibody; Sm, sphingomyelin.

administered dose. The highest cellular uptake was detected with cov-RI-PA-LIP (Figure 6A).

The EP across the cell monolayers was higher for cov-RI-PA-LIP ($7.24 \pm 0.39 \times 10^{-6}$ cm/minute), compared to b/s-RI-PA-LIP ($4.97 \pm 0.51 \times 10^{-6}$ cm/minute) (Figure 6B).

For both types of LIP, the ratio between the two radiotracers, either uptaken from the cells or recovered from the bottom compartment of the transwell system, was maintained constant with respect to the initial ratio.

## Assessment of LIP cytotoxicity on hCMEC/D3 cells

Cell viability after incubation with LIP was assessed by MTT assay. All the LIP preparations tested were nontoxic, since the cell viability did not decrease below 96% (data not shown). Moreover, after hCMEC/D3 incubation with LIP, the TEER value and the permeability of [$^{14}$C]-sucrose ($119 \pm 8\ \Omega \cdot cm^2$ and $1.62 \times 10^{-3}$ cm/minute, respectively) did not change within the experimental error ($<3\%$).
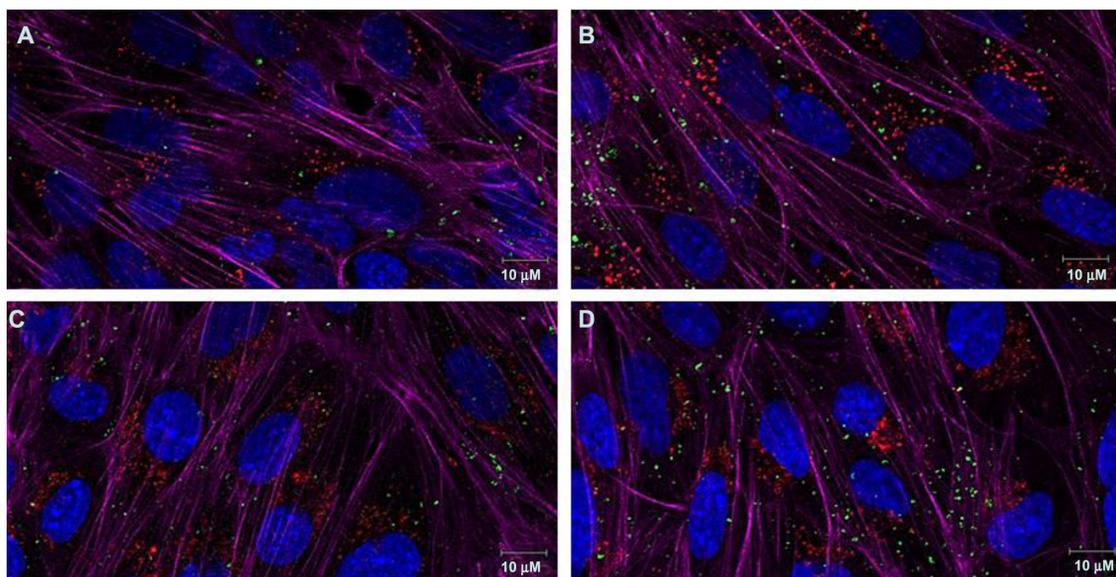


**Figure 5** CLSM of hCMEC/D3 cells after incubation with RI-PA-LIP. hCMEC/D3 cells were incubated with fluorescent-labeled cov-RI-PA-LIP (200 nmols of total lipids) at 37°C, 5% $CO_2$ saturation. hCMEC/D3 cells after (**A**) 2 hours or (**B**) overnight incubation with LIP and EAA1; hCMEC/D3 cells after (**C**) 2 hours or (**D**) overnight incubation with LIP and LAMP1.
**Notes:** Cells were incubated with phalloidin in order to visualize the actin filaments (magenta fluorescence); nuclear staining was performed by DAPI (blue staining). Early endosome staining was performed by anti-EAA1 antibodies (red fluorescence; **A** and **B**). Late endosome/early lysosomes staining was performed by anti-LAMP1 antibodies (red fluorescence; **C** and **D**) and BODIPY-Sm to mark LIP (green staining). Scale bar = 10 μM.
**Abbreviations:** BODIPY, boron-dipyrromethene; CLSM, ; cov, covalent; DAPI, 4′,6-diamidino-2-phenylindole; LAMP1, lysosomal-associated membrane protein 1; LIP, liposomes; PA, phosphatidic acid; CLSM, confocal laser scanning microscopy; RI, anti-transferrin RI7217; Sm, sphingomyelin.
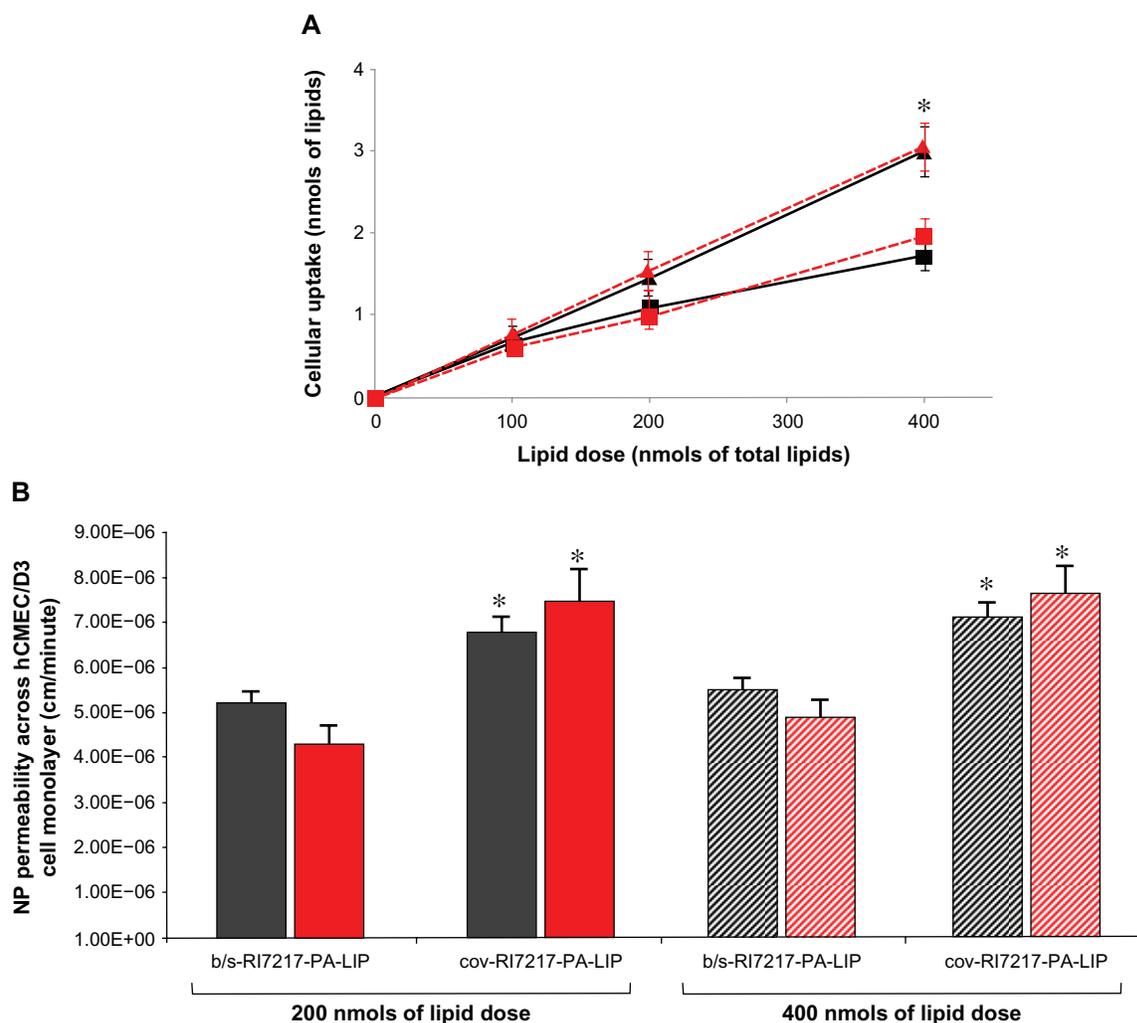
**Figure 6** Cellular uptake and permeability of LIP by hCMEC/D3 cell monolayers. $10^6$ cells were incubated with dual-radiolabeled RI-PA-LIP for 2 hours at 37°C, 5% $CO_2$. (**A**) Cellular uptake of RI-PA-LIP. After incubation, the amount of radioactivity incorporated into the cells was measured and the nmols of total lipids uptaken from the cells calculated for b/s-RI-PA-LIP (squares) or cov-RI-PA-LIP (triangles), for both radiotracers used ([$^3$H]-Sm, black; [$^{14}$C]-PA, red). (**B**) Transcytosis of RI-PA-LIP through hCMEC/D3 cell monolayers. Dual-radiolabeled LIP were added to the upper chamber of the transwell monolayers and incubated for 120 minutes at 37°C, 5% $CO_2$. The permeability of LIP across the cell monolayer was calculated for both radiotracers used, [$^3$H]-Sm (dark bars) and [$^{14}$C]-PA (red bars).
**Notes:** Each value is the mean of at least three independent experiments and the SDs of means are presented as bars. *$P < 0.05$.
**Abbreviations:** b/s, biotin/streptavidin; cov, covalent; LIP, liposomes; PA, phosphatidic acid; RI, RI7217 antibody; Sm, sphingomyelin.

# Discussion

Among several nanoparticles available, LIP have many advantages for drug delivery, due to their nontoxic and nonimmunogenic, fully biodegradable, and structurally versatile nature.[28] In this study, we functionalized PA-LIP, which already demonstrated high affinity for Aβ,[10] with the antibody RI7217 against TfR, as a candidate ligand for enhancing BBB crossing. We utilized the human brain capillary endothelial cell line hCMEC/D3, expressing TfR,[27] cultured on a transwell system, as an in vitro model of BBB.

Among the possible ligands for TfR,[19,29,30] anti-TfR RI7217 monoclonal antibody was employed for LIP decoration, for different reasons. First, the use of transferrin for decoration was discarded, because it would compete with the endogenous circulating molecule in vivo.[31] Secondly,

RI7217, in spite of being an anti-mouse antibody, has been reported to associate in vitro with human TfR, probably due to the 86% homology between mouse and human receptor.[32] Moreover, it has been shown to significantly enhance the brain uptake of LIP in vivo.[33]

We decorated PA-LIP with RI7217 using two techniques, biotin/streptavidin ligation and thiol–maleimide covalent coupling, then examined LIP performance in terms of ability to bind Aβ or TfR, cellular uptake, and permeability across a monolayer of hCMEC/D3 cells. Preparation conditions were optimized to obtain a given number of RI7217 molecules exposed on the LIP surface (40–45 antibodies/LIP) with each technique. This density was previously suggested to be optimal for brain targeting using LIP functionalized with a similar anti-TfR antibody.[33] Since the chemical

modifications on RI7217 occur randomly on primary amino groups, the antigen-binding regions could also be affected, thus causing the antibody to lose activity.[34,35] We verified by immunoblotting that the modifications on RI7217 (either biotinylation or thiolation) do not alter its binding properties toward the receptor. We also disclosed, either by immunoblotting or by SPR techniques, that both cov-RI-PA-LIP and b/s-RI-PA-LIP efficiently bind TfR, proving the efficacy of both coupling methods. In particular, SPR registered higher affinity values for cov-RI-PA-LIP, in comparison to b/s-RI-PA-LIP.

Successively, SPR indicated that RI7217 functionalization, for both types of LIP, did not modify the binding properties of PA, which maintains the affinity towards fibrillar Aβ peptide in the nanomolar range, in close agreement with data previously reported.[10] It would also be interesting to assess the affinity for oligomers (considered to be the most toxic species of the peptide), but currently this feature can be estimated only imprecisely by this technique.[10]

We demonstrated that the presence of RI7217 on the surface enhanced the cellular uptake and permeability of PA-LIP on hCMEC/D3 BBB model, with no alterations in cell viability and monolayer integrity. Confocal microscopy experiments illustrated that RI-PA-LIP are not transported via the endosome–lysosome pathway, suggesting receptor-mediated transcytosis as a possible transport mechanism across the hCMEC/D3 monolayer, as already suggested in literature on RI7217-nanoparticles.[36] This mechanism involves the activation of TfR signaling pathway and the participation of Rab proteins and PI(3)K in the regulation of vesicular trafficking. It has been suggested that, by utilizing specific inhibitors of the intracellular sorting and recycling pathways of TfR, one can switch from recycling to transcytosis and maximize the transcellular delivery of therapeutics.[37] It will be interesting to investigate this possibility with nanocarriers.

No cytotoxicity towards hCMEC/D3 cells of all LIP tested was found, indicating their likely biocompatible features. Moreover, we investigated the influence of the coupling procedure on the LIP ability to be internalized by endothelial cells and to cross the BBB model, and we found that the performance of cov-RI-PA-LIP was better than b/s-RI-PA-LIP. It could be noted that the higher permeability of cov-RI-PA-LIP does not exactly match their much higher binding affinity. Since the mechanism by which RI7217-functionalized LIP enter the cells is likely receptor-mediated, we speculate that these differences could be due to the very large bulk of the streptavidin–biotin bridge between RI7217 and LIP, in comparison to the covalent

linkage, dampening the internalization. The results proved that double radiolabeled RI-PA-LIP were likely transported intact across the hCMEC/D3 monolayer, as the ratio between the two radiotracers did not change in the upper and lower compartments of the transwell system. Taken all together, our results demonstrate that the chemical design affects the biological properties of RI-PA-LIP. In particular, PA-LIP functionalized with the RI7217 by covalent coupling are the best performing in terms of permeability across this BBB mode. Taking also into account the potential immunogenicity of streptavidin in vivo,[38] our results, obtained in vitro, suggest that the covalent bond could be adequate for the design of nanosystems able to bind Aβ and cross the BBB for AD treatment. Concerning the future use in vivo, a number of questions remain. For instance, regarding the fate of liposome–amyloid complex, and whether the liposome binding could facilitate the Aβ scavenge and degradation in the cells; whether binding to Aβ will still be efficient and specific; and whether RI-PA-LIP will be stable in the brain where high Aβ concentrations are present. All these issues deserve more experimental efforts and should be evaluated in vivo.

## Conclusion

The present in vitro study shows that LIP containing PA and decorated with RI7217 could be interesting nanosystems for further studies to develop effective strategies to treat AD. Moreover, our results provide evidence that the covalent coupling methodology could be preferable over the biotin/streptavidin method, at least under the experimental conditions adopted, for constructing RI-PA-LIP with the aim to cross the BBB.

## Acknowledgments

## Disclosure

The authors report no conflicts of interest in this work.

## References

1. Hampel H, Prvulovic D, Teipel S, et al; German Task Force on Alzheimer's Disease (GTF-AD). The future of Alzheimer's disease: the next 10 years. *Prog Neurobiol*. 2011;95(4):718–728.

2. Serrano-Pozo A, Frosch MP, Masliah E, Hyman BT. Neuropathological alterations in Alzheimer disease. *Cold Spring Harb Perspect Med*. 2011;1(1):a006189.

3. Palmer AM. The role of the blood brain barrier in neurodegenerative disorders and their treatment. *J Alzheimers Dis*. 2011;24(4):643–656.

4. Patel MM, Goyal BR, Bhadada SV, Bhatt JS, Amin AF. Getting into the brain: approaches to enhance brain drug delivery. *CNS Drugs*. 2009;23(1):35–58.

5. Craparo EF, Bondì ML, Pitarresi G, Cavallaro G. Nanoparticulate systems for drug delivery and targeting to the central nervous system. *CNS Neurosci Ther*. 2011;17(6):670–677.

6. Costantino L. Drug delivery to the CNS and polymeric nanoparticulate carriers. *Future Med Chem*. 2010;2(11):1681–1701.

7. Brambilla D, Le Droumaguet B, Nicolas J, et al. Nanotechnologies for Alzheimer's disease: diagnosis, therapy, and safety issues. *Nanomedicine*. 2011;7(5):521–540.

8. Re F, Gregori M, Masserini M. Nanotechnology for neurodegenerative disorders. *Maturitas*. 2012;73(1):45–51.

9. Re F, Moresco M, Masserini M. Nanoparticles for neuroimaging. *J Phys D Appl Phys*. 2012;45:3001–3012.

10. Gobbi M, Re F, Canovi M, et al. Lipid-based nanoparticles with high binding affinity for amyloid-β 1-42 peptide. *Biomaterials*. 2010;31(25):6519–6529.

11. Bereczki E, Re F, Masserini ME, Winblad B, Pei JJ. Liposomes functionalized with acidic lipids rescue Aβ-induced toxicity in murine neuroblastoma cells. *Nanomedicine*. 2011;7(5):560–571.

12. Qian ZM, Li HY, Sun HZ, Ho K. Targeted drug delivery via the transferrin receptor-mediated endocytosis pathway. *Pharmacol Rev*. 2002;54(4):561–587.

13. Moos T, Rosengren NT, Skjørringe T, Morgan EH. Iron trafficking inside the brain. *J Neurochem*. 2007;103(5):1730–1740.

14. Manjappa AS, Chaudhari KR, Venkataraju MP, et al. Antibody derivatization and conjugation strategies: Application in preparation of stealth immunoliposome to target chemotherapeutics to tumor. *J Control Release*. 2011;150(1):2–22.

15. Liu Y, Cheng D, Liu X, et al. Comparing the intracellular fate of components within a noncovalent streptavidin nanoparticle with covalent conjugation. *Nucl Med Biol*. 2012;39(1):101–107.

16. Hansen CB, Kao GY, Moase EH, Zalipsky S, Allen TM. Attachment of antibodies to sterically stabilized liposomes: evaluation, comparison and optimization of coupling procedures. *Biochim Biophys Acta*. 1995;1239(2):133–144.

17. Stewart JC. Colorimetric determination of phospholipids with ammonium ferrothiocyanate. *Anal Biochem*. 1980;104(1):10–14.

18. Markoutsa SGE, Pampalakis G, Niarakis A, et al. Uptake and permeability studies of BBB-targeting immune-LIP using the hCMEC/D3 cell line. *Eur J Pharm Biopharm*. 2011;77(2):265–274.

19. Huwyler J, Wu D, Pardridge WM. Brain drug delivery of small molecules using immunoliposomes. *Proc Natl Acad Sci U S A*. 1996;93(24):14164–14169.

20. Ellman GL. Tissue sulfhydryl groups. *Arch Biochem Biophys*. 1959;82(1):70–77.

21. Bradford MM. A rapid and sensitive method for the quantitation of microgram quantities of protein utilizing the principle of protein-dye binding. *Anal Biochem*. 1976;72:248–254.

22. Re F, Sesana S, Barbiroli A, et al. Prion protein structure is affected by pH-dependent interaction with membranes: a study in a model system. *FEBS Lett*. 2008;582:215–220.

23. Salvati E, Masserini M, Sesana S, Sonnino S, Re F, Gregori M. Liposomes functionalized with GT1b ganglioside with high affinity for amyloid beta-peptide. *J Alzheimers Dis*. 2012;29(Suppl 1):33–36.

24. Re F, Cambianica I, Sesana S, et al. Functionalization with ApoE-derived peptides enhances the interaction with brain capillary endothelial cells of liposomes binding amyloid-beta peptide. *J Biotechnol*. 2010;156(4):341–346.

25. Cecchelli R, Dehouck B, Descamps L, et al. In vitro model for evaluating drug transport across the blood–brain barrier. *Adv Drug Deliv Rev*. 1999;36(2–3):165–178.

26. Re F, Cambianica I, Zona C, et al. Functionalization of liposomes with ApoE-derived peptides at different density affects cellular uptake and drug transport across a blood-brain barrier model. *Nanomedicine*. 2011;7(5):551–559.

27. Poller B, Gutmann H, Krähenbühl S, et al. The human brain endothelial cell line hCMEC/D3 as a human blood-brain barrier model for drug transport studies. *J Neurochem*. 2008;107(5):1358–1368.

28. Torchilin VP. Recent advances with liposomes as pharmaceutical carriers. *Nat Rev Drug Discov*. 2005;4(2):145–160.

29. Bickel U, Yoshikawa T, Pardridge WM. Delivery of peptides and proteins through the blood-brain barrier. *Adv Drug Deliv Rev*. 2001;46(1–3):247–279.

30. Kissel K, Hamm S, Schulz M, Vecchi A, Garlanda C, Engelhardt B. Immunohistochemical localization of the murine transferrin receptor (TfR) on blood-tissue barriers using a novel anti-TfR monoclonal antibody. *Histochem Cell Biol*. 1998;110(1):63–72.

31. Lee HJ, Engelhardt B, Lesley J, Bickel U, Pardridge WM. Targeting rat antimouse transferrin receptor monoclonal antibodies through blood–brain barrier in mouse. *J Pharmacol Exp Ther*. 2000;292(3):1048–1052.

32. Wang E, Obeng-Adjei N, Ying Q, et al. Mouse mammary tumor virus uses mouse but not human transferrin receptor 1 to reach a low pH compartment and infect cells. *Virology*. 2008;381(2):230–240.

33. van Rooy I, Mastrobattista E, Storm G, Hennink WE, Schiffelers RM. Comparison of five different targeting ligands to enhance accumulation of liposomes into the brain. *J Control Release*. 2011;150(1):30–36.

34. Béduneau A, Saulnier P, Hindré F, Clavreul A, Leroux JC, Benoit JP. Design of targeted lipid nanocapsules by conjugation of whole antibodies and antibody Fab' fragments. *Biomaterials*. 2007;28(33):4978–4990.

35. Ji T, Muenker MC, Papineni RVL, Harder JW, Vizard DL, McLaughlin WE. Increased sensitivity in antigen detection with fluorescent latex nanosphere-IgG antibody conjugates. *Bioconjug Chem*. 2010;21(3):427–435.

36. Wang J, Tian S, Petros RA, Napier ME, Desimone JM. The complex role of multivalency in nanoparticles targeting the transferrin receptor for cancer therapies. *J Am Chem Soc*. 2010;132(32):11306–11313.

37. Widera A, Norouziyan F, Shen WC. Mechanisms of TfR-mediated transcytosis and sorting in epithelial cells and applications toward drug delivery. *Adv Drug Deliv Rev*. 2003;55(11):1439–1466.

38. Paganelli G, Chinol M, Maggiolo M, et al. The three-step pretargeting approach reduces the human anti-mouse antibody response in patients submitted to radioimmunoscintigraphy and radioimmunotherapy. *Eur J Nucl Med*. 1997;24(3):350–351.